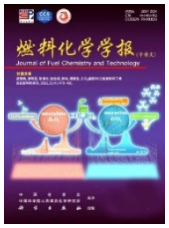

燃料化学学报(中英文)
Journal of Fuel Chemistry and Technology
ISSN 2097-213X,CN 14-1410/TQ

《燃料化学学报(中英文)》网络首发论文

题目： CHA 结构分子筛上甲醇与长链烷烃耦合反应（英文）
作者： 杨闯，王康军，李金哲，刘中民
收稿日期： 2025-03-27
网络首发日期： 2025-09-29
引用格式： 杨闯，王康军，李金哲，刘中民．CHA 结构分子筛上甲醇与长链烷烃耦合反应（英文）[J/OL]．燃料化学学报(中英文).
https://link.cnki.net/urlid/14.1410.TQ.20250928.1719.003

JOURNAL OF FUEL CHEMISTRY AND TECHNOLOGY
Volume 54, Issue 2, February 2026

燃料化学学报(中英文) Journal of Fuel Chemistry and Technology

Cite this article as: J Fuel Chem Technol, 2026, 54, 20250054

Coupling of methanol and long chain alkanes on molecular sieves with CHA structures

YANG Chuang[1,2], WANG Kangjun[1,*], LI Jinzhe[1,2,*], LIU Zhongmin[1,2,*]

[1] College of Chemical Engineering, Shenyang University of Chemical Technology, Shenyang 110142, China;
[2] National Engineering Research Center of Lower-Carbon Catalysis Technology, Dalian Institute of Chemical Physics, Chinese Academy of Sciences, Dalian 116023, China

Abstract: The coupling reactions of methanol and long-chain alkanes (n-dodecane, n-tetradecane and n-hexadecane) over CHA-type molecular sieves were studied in a fixed bed reactor. Over SAPO-34 and SSZ-13, it was found that the induction period of methanol conversion was shortened by the introduction of long-chain alkanes. However, the addition of long-chain alkanes had little influence on the product distribution. Polymethylbenzenes and the derivatives were the main retained species on spent SSZ-13 catalyst, while adamantanes were the main retained species on SAPO-34. This indicates that coking species formation was mainly related to the further transformation of long-chain alkane/methanol coupling products at acid sites of the molecular sieve. These findings provide valuable information of long chain alkanes conversion and methanol reaction behavior of induction period over small pore CHA molecular sieves.

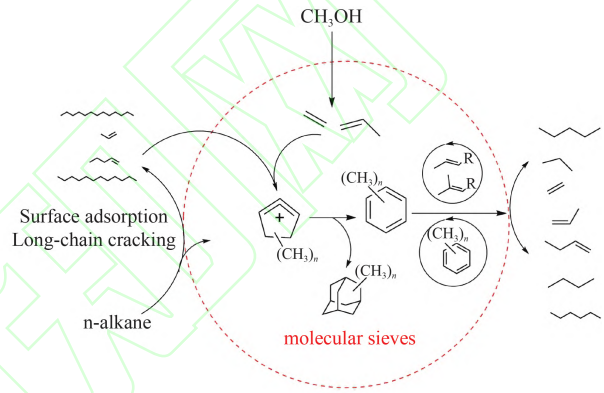

Key words: Methanol; Long-chain alkane; Coupling transformation; Induction period; Molecular sieves

In the catalytic reactions over molecular sieves, the reaction phenomena and obtained results are affected by the reaction conditions and the molecular sieve configuration. The topological structure, the size of pore-openings and the acid sites property were the most important factors. As a promising process for producing gasoline, light olefins and aromatics from non-petroleum carbon sources, the conversion of methanol to hydrocarbons (MTH) on zeolites or zeolite-based materials has attracted numerous studies and increasing attention over the past decades.[1−8] Among the reported catalysts, CHA-type molecular sieves (e.g., SAPO-34 and SSZ-13) exhibited very high light olefins selectivity and SAPO-34 was the catalyst in the commercial methanol-to-olefins (MTO) process. The 8-membered-ring small pores and supercages of CHA molecular sieves define their unique pore structure. The 8-membered-ring windows restrict macromolecule diffusion via shape selectivity, allowing only small molecules to pass while inhibiting coke precursors formation. As three-dimensionally interconnected cavities, the supercage provide confined reaction spaces that host aromatic hydrocarbon intermediates in the hydrocarbon pool mechanism, enabling gradual methanol dehydration and alkylation at the acid sites to form olefins. The synergy between dynamic intermediate evolution in supercages and product diffusion control by small pores ensures high olefin selectivity, establishing CHA as an ideal catalytic structure for MTO. Notably, CHA topology is among the few frameworks allowing synthesis of both silicoaluminophosphate (SAPO) and aluminosilicate (SSZ-13) analogs. Studies demonstrate that H-SSZ-13 exhibits higher acid strength than H-SAPO-34.[9] Liang et al.[10−11] from the Dalian Institute of Chemical Physics first reported SAPO-34 catalytic application in MTO, observing 90% C_2-C_4 olefin selectivity at near-complete methanol conversion, with retained high activity after 55 regeneration cycles. Owing to its balanced acidity

Received: 2025-03-27; Revised: 2025-04-17
Foundation items: Supported by National Natural Science Foundation of China (21991093).
* Corresponding author. E-mail: wangkj_dut@syuct.edu.cn, lijinzhe@dicp.ac.cn, iuzm@dicp.ac.cn.
CSTR: 32157.14.2097-213X.2025.JFCT.0147
本文的英文电子版由 Elsevier 出版社在 ScienceDirect 上出版 (http://www.sciencedirect.com/science/journal/18725813)

and pore structure, SAPO-34 outperforms SSZ-13 in low-carbon olefin selectivity during MTO[11−15]. Through years of development, Dalian Institute of Chemical Physics has developed a series of methanol-to-olefins (DMTO) technologies based on fluidized bed processes. Currently, DMTO-Ⅲ has been applied in actual production. Furthermore, it was found that when SAPO-34 molecular sieve was used in the methanol conversion reaction, different reaction characteristics manifested at high and low temperatures[16−20]. Low-temperature reactions have the characteristics of a definite induction period and rapid deactivation.

These findings deepen our understanding of MTO mechanism and benefit the catalyst design and process development. However, it is still difficult to tune the product selectivity and coke formation during the induction period. The reaction mechanism of induction period remains to be clarified. Based on the previous studies of methanol conversion over CHA (SAPO-34/SSZ-13)[21], this work introduces long-chain alkanes with methanol to investigate the coupling effects and the mechanisms during induction period. Given CHA's pore structure, large long-chain hydrocarbons cannot diffuse into the CHA molecular sieve interior. However, it was found that long-chain alkanes could improve the conversion of methanol over SAPO-34 and SSZ-13. By comparing SAPO-34 and SSZ-13 in alkane-methanol coupling reactions, we explore intrinsic induction period behaviors and molecular sieve-specific catalytic differences.

1 experimental

1.1 catalysts

The SAPO-34 and SSZ-13 used in the experiments were obtained from the Catalyst Factory of Nankai University. The catalyst powders were pressed into tablets, crushed and sieved into 20−40 mesh for the experiment.

1.2 Characterization of the catalysts

The XRD patterns of the powder were recorded by using the PANalytical X'Pert PRO X-ray diffractometer under Cu-*K*α radiation (λ=1.54059 A) at 40 kV and 40 mA with a range of 5°−90° and a scanning speed of 5(°)/min. The chemical composition of the sample was determined by using the Philips Magix-601 X-ray fluorescence (XRF) spectrometer at a voltage of 40 kV and a current of 40 mA. The crystal morphology and structure were observed by field emission scanning electron microscopy (Hitachi, SU8020). Physical adsorption and desorption were determined using the Micrometrics ASAP 2020 system with N_2 as the adsorption gas at the temperature of liquid nitrogen (77 K). The specific surface area of the sample was determined by the BET formula, and the total pore volume of the sample was calculated based on the adsorption amount of N_2 when the relative pressure was 0.97. The surface area and pore volume of micropores were calculated by using the *t*-plot method. The calcined samples were activated and treated for 40 minutes in a He atmosphere at 600 ℃ and 40 mL/min by the method of programmed temperature desorption of ammonia (NH_3-TPD). After the temperature dropped to 100 ℃, NH_3 was injected to saturate the adsorption of the sample. The physically adsorbed NH_3 was blown away by He, and then the temperature was programmed at a rate of 10 ℃/min to 600 ℃. The desorption signal was recorded by the TCD detector, and its acidity was investigated.

1.3 Catalytic studies

The conversion of methanol and long-chain alkanes was carried out in a fixed-bed reactor, using a quartz tube microreactor with an inner diameter of 6mm. Press the catalyst into tablets, crush them and then sieve them into 20−40 mesh. All experiments used 0.1 g of catalyst samples. The typical reaction process is described as follows: Take the molecular sieve catalyst sample required for the experiment and put it into a quartz tube. The carrier gas is passed through the reactor and heated to 550 ℃ for activating the catalyst for 30 minutes, and then cooled down to the required experimental temperature to start the reaction. The mass space velocity of methanol is 3.39g/(g·h), and the partial pressure of methanol is 17.13 kPa. The content of alkanes in methanol was calculated using the carbon mole percent. The products was analyzed online using gas chromatography (Agilent GC 8890A). Analysis conditions: Hydrogen flame ionization detector (FID), HP-1 capillary chromatographic column, column oven temperature programmed from 40 ℃ to 300 ℃. The methanol conversion and product selectivity is calculated based on CH_2 and dimethyl ether is considered as the reactant.

The raw materials and reagents used in the experiments include methanol (analytical grade, Guangdong Guanghua Science & Technology Co., LTD.), n-dodecane (analytical grade, Aladdin Reagent Co., LTD.), n-tetradecane (analytical grade, Aladdin Reagent Co., LTD.), n-hexadecane (analytical grade, Aladdin Reagent Co., LTD.), and dichloromethane (analytical grade, Guangdong Guanghua Science and Technology Co., LTD.), hexachloroethane (chemically pure, Aladdin Reagent Co., LTD.), hydrofluoric acid (40%, Tianjin Damao Chemical Reagent Factory).

1.4 Extraction and GC-MS analysis of the retained species

The retained species on the catalyst after the reaction were analyzed by dissolving the spent catalyst (100 mg) in 1.0 mL 40% HF in a screw-capped Teflon-lined vial to obtain the organic compounds trapped in the catalyst. The

organic phase was extracted by CH_2Cl_2 and then analyzed by Agilent 7890A/5975C GC/MSD.

2 Results and discussion

2.1 Characterization of the catalysts

The XRD results show that both SAPO-34 and SSZ-13 samples have typical CHA-type topological structures.

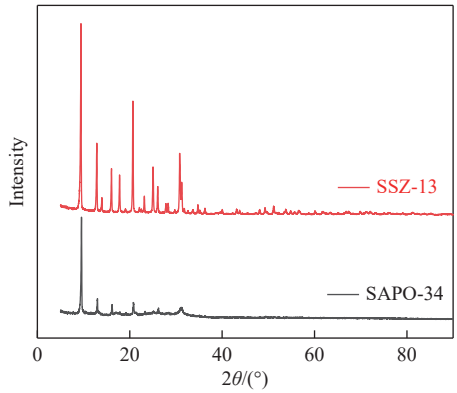

Fig. 1 XRD of SAPO-34 sample and SSZ-13 sample

The SEM characterization results are shown in Figure 2. The SAPO-34 sample has a typical cubic structure with a particle size of 2−3 μm. SSZ-13 has a spheroid structure with a particle size of 1-2μm. Both have a relatively high degree of crystallinity. The Si/(Si+Al+P) ratio of the SAPO-34 sample was characterized as 0.11 by elemental analysis (XRF), and the Si/Al ratio of the SSZ-13 sample was 11.

The physical adsorption results of N_2 for samples with different structures show that both samples have typical microporous structures. The specific surface area and pore volume of the samples are listed in Table 1.

The results of NH_3-TPD in samples of catalysts with different structures are shown in Figure 3. There are two type acid sites of different intensities on the selected samples: the weak acid site at 150−300 ℃ and the strong acid site at 300−600 ℃. However, the acid strength of the SSZ-13 sample is higher than that of the SAPO-34 sample. The acid density of the SSZ-13 sample is higher than that of the SAPO-34 sample. Through quantitative calculation, the acid content on the SAPO-34 catalyst was 0.97 mmol/g, and that on the SSZ-13 catalyst was 1.12 mmol/g.

2.2 Methanol and alkane co-feeding

Combined with the mechanism research in literature[22], the coupling reaction of methanol and long-chain alkanes over SAPO-34 and SSZ-13 was investigated at 250 ℃. In the pre-experiment stage, the methanol conversion on the catalysts was examined and the results are shown in Figure 4. The SAPO-34 exhibited a typical induction period characteristic with methanol conversion gradually increases to 4.83%, demonstrating distinct autocatalytic behavior. In contrast, SSZ-13 showed rapid activation characteristics, achieving an initial conversion of 0.169% at 5 min and a maximum conversion of 22.08% at 48 min, followed by rapid deactivation. The product over the SAPO-34 catalyst (Figure 4(b)) is dominated by the C_1-C_3 component, and high propylene selectivity is observed. As the reaction proceeded, the C_4-C_6 products were detected. Product selectivity over the SSZ-13 catalyst (Figure 4(c)) revealed that the main products are methane and C_2-C_3 alkenes, among which the selectivity of propylene reaches the maximum value at the highest methanol conversion point. It is worth noting that the generation of C_6 alkanes were detected at the maximum conversion. The product distribution in the deactivation stage showed significant changes: the selectivity of butene and pentane increased, but the ratio of propylene/ethylene was still greater than 1. The similar product distributions on the two catalysts indicate that the distribution of acidic sites and the pore structure have similar restrictive effects on the product distribution.

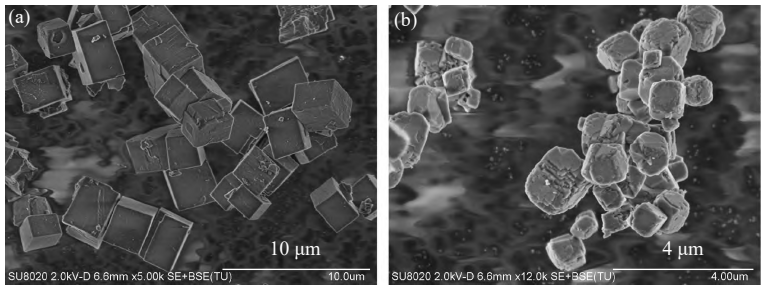

Fig. 2 SME results of SAPO-34 (a) and SSZ-13(b)

Table 1 N_2 physical adsorption results of SAPO-34 and SSZ-13 samples

sample	S_{BET}/($m^2 \cdot g^{-1}$)	S_{micro}/($m^2 \cdot g^{-1}$)[a]	S_{ext}/($m^2 \cdot g^{-1}$)[a]	v_{total}/($mL \cdot g^{-1}$)[b]	v_{micro}/($mL \cdot g^{-1}$)[c]
SAPO-34	290	282	7.28	0.23	0.15
SSZ-13	521	517	4.57	0.31	0.27

[a]: *t*-plot micropore and external surface area; [b]: Volume adsorbed at $p/p_0 = 0.97$; [c]: *t*-plot micropore volume.

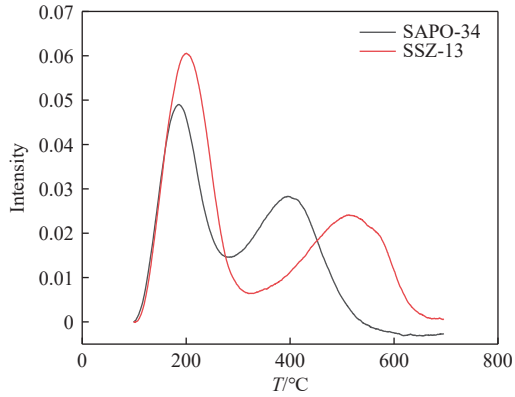

Fig. 3 NH_3-TPD of SAPO-34 sample and SSZ-13 sample

However, divergent reaction pathways became evident in the deactivation stage.

The effect of long chain alkanes on methanol conversion over SAPO-34 and SSZ-13 were studied by co-feeding long chain alkanes with methanol. It was determined that the maximum solubility of n-hexadecane in methanol was 3% C-mol at 25 ℃. To clarify product distribution patterns during the induction period and probe hydrocarbon pool evolution, experiments employed 1% C-mol co-fed long-chain alkanes-well below the saturation limit. The co-feeding reactions were carried out at 250 ℃. Figure 5 demonstrates time-dependent methanol conversion and product selectivity evolution on SAPO-34 under these co-feeding conditions.

As shown in Figure 5(a), co-feeding hexadecane significantly increased methanol conversion, achieving a maximum conversion of 8.64%-double that of the methanol-only system. Product selectivity profiles are shown in Figure 5(b)−(d). Over SAPO-34, only C_2-C_3 olefins were detected initially. With reaction progression, a methane/ethylene/propylene-dominated distribution emerged, maintaining propylene/ethylene selectivity ratios >1. Notably, while alkane co-feeding shortened the induction period and accelerated reaction, the product distribution is similar with methanol feeding. This demonstrates SAPO-34's channel shape-selective dominance in product control.

Figure 6 shows the variation patterns of methanol conversion and product selectivity with reaction time of SSZ-13 under the co-feeding conditions of methanol and 1% C-mol long-chain alkanes. As shown in Figure 6(a), the methanol conversion of each system exhibited a unimodal conversion characteristic (initial increase followed by decline). The methanol and tetradecane co-feeding system achieved peak conversion of 50.51% – 2.3-fold higher than methanol-only feeding (22.09%). Notably, unlike SAPO-34's general alkane promotion effect, the SSZ-13 system demonstrates a significant methanol conversion promoting

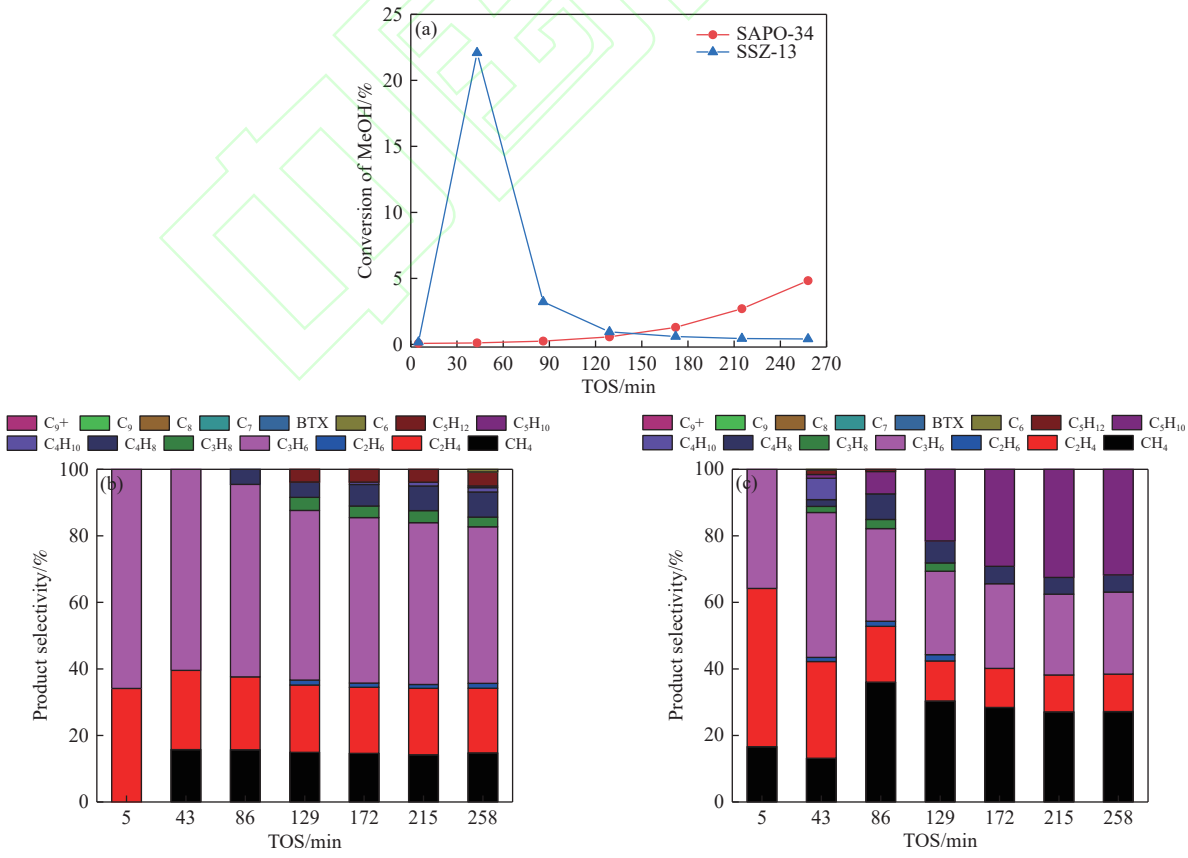

Fig. 4 Methanol over CHA type molecular sieves. (a) methanol conversion, (b) product selectivity on SAPO-34, (c) product selectivity on SSZ-13. (Reaction conditions: Reaction temperature =250 ℃, Methanol mass space velocity =3.39g/(g·h), Methanol partial pressure =17.13kPa)

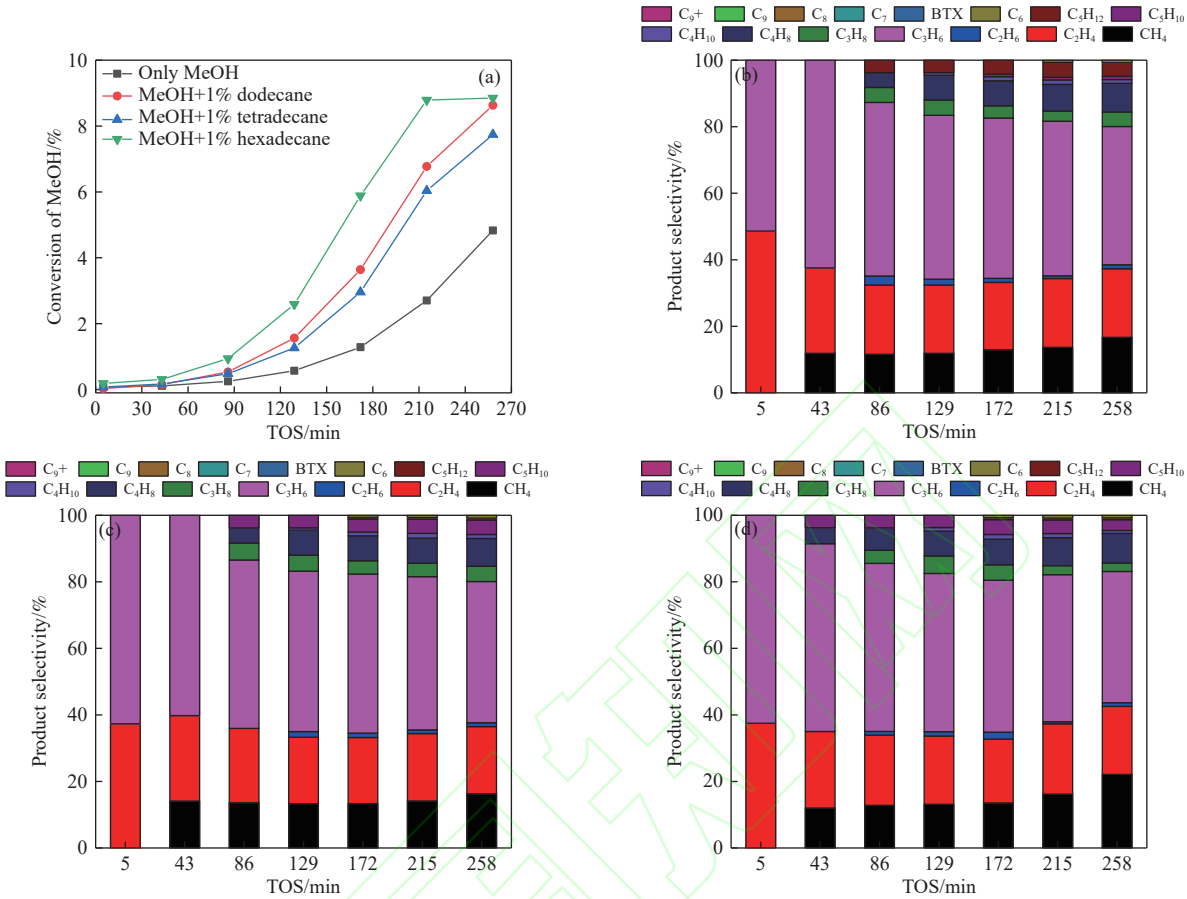

Fig. 5 Co-feeding 1% C-mol long chain alkanes with methanol over SAPO-34. (a) methanol conversion, (b) product selectivity of co-feeding dodecane and methanol, (c) product selectivity of co-feeding tetradecane and methanol, (d) product selectivity of co-feeding hexadecane and methanol. (Reaction conditions: Reaction temperature =250 ℃, mass space velocity =3.39g/(g·h), partial pressure of methanol =17.13 kPa)

effect in tetradecane, potentially linked to its unique microporous framework and acidic properties. Product selectivity analysis (Figure 6(b)−(d)) revealed initial methane/C2-C3 hydrocarbon dominance, with the propylene/ethylene ratio always remains above 1. Over time, the formation of C_4-C_6 low-carbon olefins was gradually detected. During the catalyst deactivation stage, the product distribution evolves towards the concentration of C_2, C_3 and C_5 hydrocarbons. Crucially, alkane co-feeding did not alter SSZ-13's product distribution patterns or key alkene selectivities, indicating that the pore restriction effect dominated the reaction pathway and did not significantly induce the generation of new reaction pathways.

In contrast to reactions on SAPO-34, reactions on SSZ-13 proceed through the entire process from initiation to deactivation, making it challenging to precisely determine the impact of long-chain alkane introduction on the methanol induction period. To address this, the reaction temperature was lowered for further investigation (Figure 7(a)). With the decrease of the reaction temperature, the methanol reaction on the SSZ-13 molecular sieve slowed down, none of which reached the reaction peak except at 240 ℃, and the lower the temperature, the less obvious the reaction. At 230 ℃, the effect of long-chain alkane introduction on methanol conversion was studied (Figure 7(b)). The results show that the introduction of long-chain alkanes accelerates the conversion of methanol, and the conversion shows a trend of first increasing and then decreasing. Moreover, the higher the carbon number of the alkane, the better the reaction. This confirmed that the introduction of long-chain alkanes promotes the conversion of methanol and shortens the induction period. Furthermore, the product distribution was generally consistent with that at 250 ℃.

2.3 The Transformation and Role of HCP Species

In order to verify the above speculation, the retained species on the catalyst were analyzed. The samples were taken from the catalyst after the reaction at 250 ℃(selected because SSZ-13 undergoes the complete process from initial conversion to deactivation at this temperature, allowing analysis of retained species evolution), dissolved by HF and extracted by dichloromethane. The organic substances retained by the catalyst at different reaction times were analyzed by GC-MS.

Figure 8 shows the GC-MS analysis results of the retained species of methanol at different reaction times on

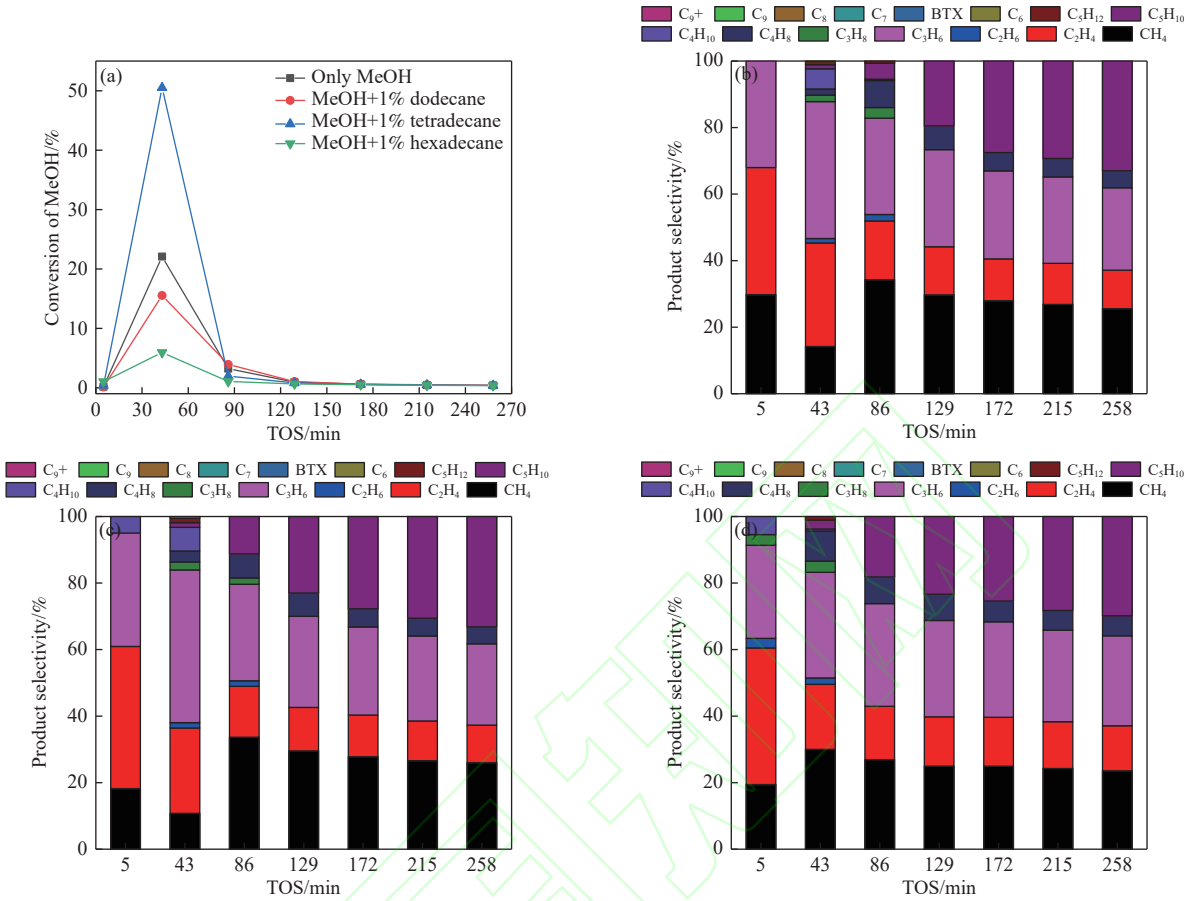

Fig. 6 Co-feeding 1% C-mol long chain alkanes with methanol over SSZ-13. (a) methanol conversion, (b) product selectivity of co-feeding dodecane and methanol, (c) product selectivity of co-feeding tetradecane and methanol, (d) product selectivity of co-feeding hexadecane and methanol. (Reaction conditions: Reaction temperature =250 ℃, mass space velocity =3.39g/(g·h), partial pressure of methanol =17.13 kPa)

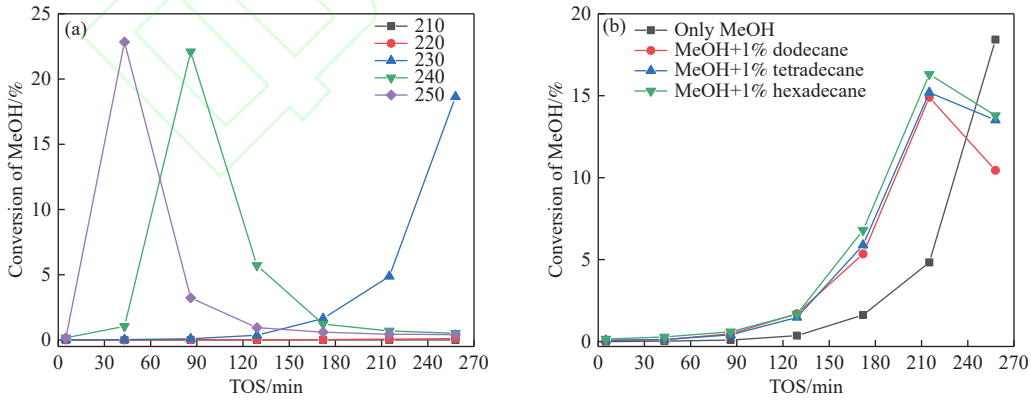

Fig. 7 Methanol conversion on SSZ-13. (a) is the conversion diagram of methanol alone reaction; (b) is the conversion diagram of methanol introducing long-chain alkanes.(Reaction conditions: Reaction temperature =230 ℃, mass space velocity =3.39g/(g·h), partial pressure of methanol =17.13 kPa)

SAPO-34 molecular sieve (Figure 8(a)) and SSZ-13 molecular sieve (Figure 8(b)). Analysis revealed that no significant retained species were detected on SAPO-34 after 30 minutes of reaction. At 60 minutes, the retained species emerged. With the increase of reaction time, the types and contents of retained species such as adamantane, cycloalkane and polymethylbenzene increased, and correspondingly, methanol was also rapidly converted. When reacting on the SSZ-13 molecular sieve for 5 minutes, no obvious retained species were observed. However, peaks could be seen at the positions of tetramethylbenzene, pentamethylbenzene, hexamethylbenzene, and adamantanes. At 30 minutes of the reaction, hexamethylbenzene content surged abruptly, and

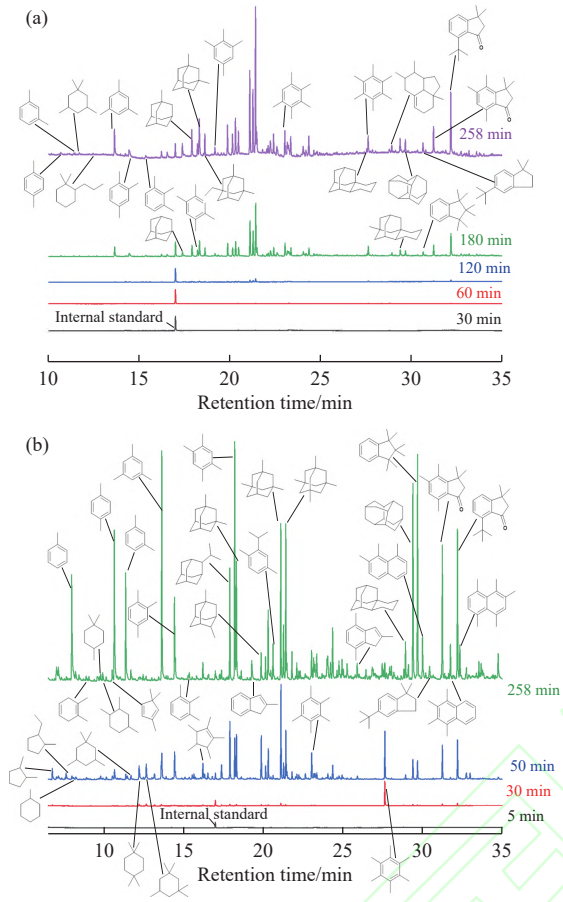

Fig. 8 GC-MS diagram of resident species with different reaction time when methanol on SAPO-34 (a) and SSZ-13 (b)

the types of adamantane also increased. At 50 minutes of the reaction, the types of retained species significantly increased and their contents increased. At this time on stream, the methanol conversion was the highest. When the molecular sieve is deactivated, hexamethylbenzene content declined, while the content of retained species such as xylenes, pentamethylbenzene, adamantanes, and naphthalene accumulated significantly. It is speculated that the retained species may clog the molecular sieve channels, leading to the deactivation of the catalyst.

Figure 9 shows the GC-MS analysis results of the retained species when 1%C-mol long-chain alkanes and methanol co-feeding and reacting on the SAPO-34 molecular sieve catalyst for 258 minutes. Analysis reveals that the types and contents of adamantane in the retained species varied with the different co-feeding alkanes. This observation aligns with previous work from our laboratory[23], which demonstrated that on the SAPO-34 molecular sieve with a cage structure, the deactivation of the low-temperature methanol-to-hydrocarbon reaction is mainly due to the generation of adamantane compounds. Overall, the retained species include polymethylbenzenes and derivatives (from xylene to hexamethylbenzene), adamantane and the methyl-substituted adamantanes, hydrocarbon species such as alkanes, cycloalkanes, and alkenes, as well as ketenes species. Among them,

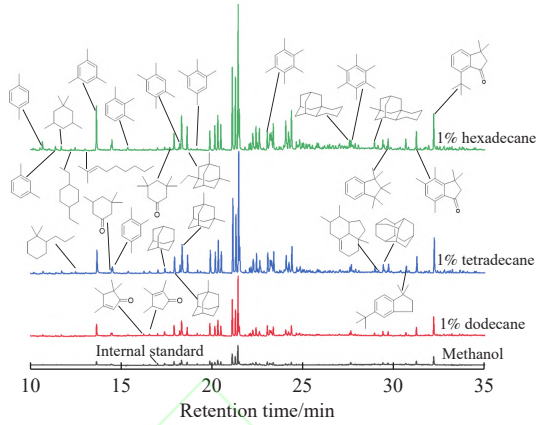

Fig. 9 GC-MS diagram of resident species on SAPO-34 after 258 minutes reaction with different raw materials

adamantane and its methyl-substituted adamantane dominate resident species. The amount of hexamethylbenzene in the retained species is very small, likely due to its high reactivity, making it difficult to capture. When hexadecane is introduced into methanol, a diverse array of adamantane derivatives with high abundance is generated. The peaks without marked structures in the GC-MS diagram (Figure 9) are all methyl-substituted adamantane peaks.

Figure 10 shows the GC-MS analysis results of the retained species during co-feeding of 1% C-mol hexadecane and methanol over the SAPO-34 molecular sieve catalyst at different reaction times. Analysis revealed that only adamantane was detected at 30 minutes. At 60 minutes of the reaction, weak signals corresponding to trimethylbenzene, tetramethylbenzene, pentamethylbenzene and hexamethylbenzene began to emerge. At 120 minutes of the reaction, the types and concentrations of the retained species increased. As the reaction time increased, the concentrations of the retained species increased significantly. Notably, adamantane and its derivatives dominated in both type and abundance throughout the reaction. According to previous reports[24], Si distribution in

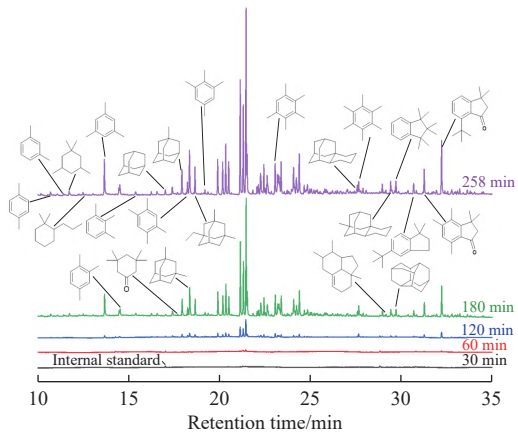

Fig. 10 GC-MS diagram of resident species with different reaction time when co-feeding 1% C-mol hexadecane with methanol over SAPO-34

SAPO-34 crystals is heterogeneous, gradually increased from inside to surface. The acid density in the cage near the outer surface of the crystal is higher, which is more conducive to the generation of retained species. Based on this, it is speculated that at low temperatures, a certain amount of inert adamantane species are first generated in the cage of SAPO-34 molecular sieve catalyst near the outer surface of the crystal, which will lead to the restriction of the diffusion of the product through the outer surface of the crystal. However, methylbenzenes in inner cages retain high reactivity, enabling continued reaction with methanol to form low-carbon olefins. As diffusion pathways through the surface become obstructed, adamantane generation within inner cages accelerates. This explains the sustained increase in methanol conversion despite progressive adamantane accumulation. Furthermore, compared to the reaction of methanol alone (Figure 8(a)), it can be found that the introduction of long-chain hydrocarbons shortens the generation time of polymethylbenzene and adamantane. Polymethylbenzene promotes the reaction, shortens the induction period, and promotes the conversion of methanol.

Figure 11 shows the GC-MS analysis results of the retained species when 1%C-mol long-chain alkanes and methanol were co-feeding on the SSZ-13 catalyst for 258 minutes. Analysis reveals that no significant differences exist in the retained species on the SSZ-13 catalyst across different raw materials. The retained species include polymethylbenzenes, naphthalenes, adamantanes, and cycloalkanes/cycloalkenes. Among them, the contents of toluene, xylene, 1,3,5-trimethylbenzene, 1,2,4-trimethylbenzene, 1,2,3,5-tetramethylbenzene, 1,1,2,3,3,5-hexamethylindene and hydronaphthalene are very high and are the main retained species. Especially, the concentration of 1,2,3,5-tetramethylbenzene exhibiting the highest concentration. The distribution of isomers of toluene, xylene, trimethylbenzene and tetramethylbenzene reflects the spatial confinement effect of the molecular sieve supercage structure. Meanwhile, pentamethylbenzene and hexamethylbenzene are present in trace amounts, likely because the reaction enters the deactivation stage, favoring the formation of larger molecules such as naphthalene. The peaks without marked structures in the GC-MS diagram of Figure 10 are all methyl-substituted adamantane peaks.

Figure 12 shows the GC-MS analysis results of the retained species during co-feeding of 1% C-mol hexadecane and methanol over the SSZ-13 molecular sieve catalyst at different reaction times. Analysis revealed that at 5 minutes, adamantane and hexamethylbenzene had already formed, though their concentrations remained low. By 30 minutes of the reaction, hexamethylbenzene content surged, and other retained species also began to form. When the reaction reached the highest conversion of 50 minutes, the contents of various retained species were all increasing, with a distribution pattern resembling that observed over deactivated catalyst. Notably, high concentrations of hexamethylbenzene, cyclopentadiene, cyclohexadiene, and enones persisted. At this time, the content of polymethylbenzene from toluene to pentamethylbenzene remained at low levels. Previous researches of our group[25] confirmed that cyclopentadiene and cyclohexadiene act as active intermediates. The high propylene yield on the SSZ-13 molecular sieve catalyst is attributed to the high reactivity of 1,2,4,5-tetramethylbenzene and hexamethylbenzene within the CHA cage. In addition, compared to the reaction of methanol alone (Figure 8(b)), it can be found that the introduction of long-chain hydrocarbons significantly accelerates polymethylbenzene and adamantane formation, increasing retained species accumulation inside the molecular sieve. Although the generation of 1,2,4,5-tetramethylbenzene and hexamethylbenzene accelerates the reaction, at the same time, the rate of transformation into species that cause molecular sieve inactivation also increases. This also corresponds to the effect of introducing long-chain alkanes on the methanol reaction (Figure 7(b)). When deactivated, the retained species showed hexamethylbenzene content sharply declined, while the contents of polymethylbenzene, naphthalene and its derivatives, indene and other species increased. It was speculated that they blocked the catalyst pores, occupied the acid sites, and led to the deactivation of

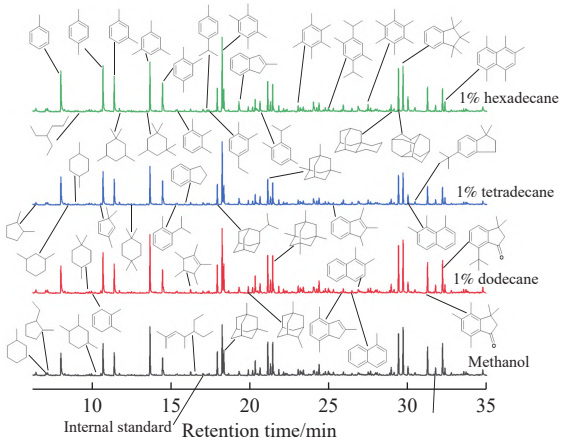

Fig. 11 GC-MS diagram of resident species on SSZ-13 after 258 minutes reaction with different raw materials

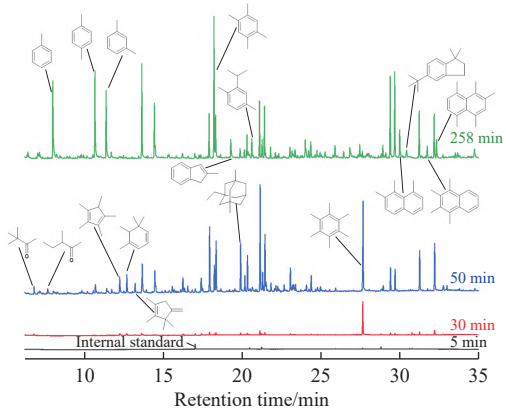

Fig. 12 GC-MS diagram of resident species with different reaction time when co-feeding 1% C-mol hexadecane with methanol over SSZ-13

the catalyst.

Because SAPO-34 and SSZ-13 have the same CHA cage to accommodate retained species, the differences in the generation of these species during the MTO reaction process may be related to the acid strength of Brønsted acid sites, which determines the protonation reaction and stability of the reaction intermediates in the catalyst cages. More precisely, the CHA cage in the SSZ-13 can provide a larger space and is more conducive to the generation of para-xylene, trimethylbenzene, and 1,2,4,5-tetramethylbenzene with larger kinetic diameters. For naphthalene and its derivatives, naphthalene and polymethyl naphthalene can be formed in the CHA cage of SSZ-13. The free space of the molecular sieve supercage shows a significant spatial limiting effect in the formation process of aromatics, including polymethyl benzene and polymethyl naphthalene. However, due to the differences in acidity (acid amount and acid strength) between SAPO-34 and SSZ-13, significant differences are shown in the generation of retained species and the promotion of reactions. Through the analysis of the retained species, it is concluded that on the SAPO-34 molecular sieve, the introduction of long-chain alkanes shortens the cyclization time and further accelerates the formation of adamantane and polymethylbenzene. Since the adamantanes are inert species and generated in the cage near the outer surface of the crystal, while the content of methylbenzene in the cage inside the crystal is low but has high reactivity. It enhance the methanol reaction to produce low-carbon olefins, accelerating the co-feeding reaction and increasing the methanol conversion. However, on the SSZ-13 molecular sieve, due to its stronger acidity and accelerated reaction rate, the formation of adamantane and polymethylbenzene has already emerged when methanol is feeding as a single component. The introduction of long-chain alkanes further intensifies the formation of adamantane and polymethylbenzene.

The shape-selective catalytic effect of molecular sieves makes the product distribution regulated by both the reaction mechanism and the diffusion coefficient. The differences in the diffusion rate and cracking performance of macromolecules significantly affect the product selectivity. According to the research and speculation of Sebastian et al.[26−27], a part of the long-chain alkanes might be cracked or directly enter the interior of the molecular sieve for cracking to generate short-chain hydrocarbons. The olefinic hydrocarbons produced by cracking are cyclized into hydrocarbon pool intermediates. Through hydrogen transfer and protonation, the dual-cycle mechanisms are accelerated, the reaction induction period is shortened, and the methanol conversion continuously increases. Due to the differences in the acidity of molecular sieves, SAPO-34 has an appropriate acidity and can effectively maintain the synergistic catalytic effect of long-chain alkanes. The reaction rate of SSZ-13 is too fast due to strong acidity, causing rapid coke deposition and deactivation. Moreover, the synergistic mechanism of alkanes is different from that of SAPO-34 and requires further exploration. Overall, the acid site distribution and strength differences of molecular sieves are the essential reasons for the differences in the co-reaction of long-chain alkanes and methanol, especially their effects on the reaction induction period and coke behavior. Figure 13 illustrates the reaction network of co-feeding long chain alkanes and methanol over CHA molecular sieves.

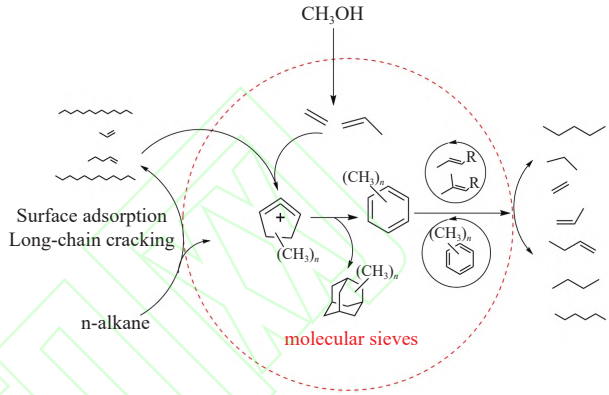

Fig. 13 Reaction network of co-feed long chain alkanes and methanol on CHA molecular sieves

2.4 3.5. Coke deposition analysis

Figure 14(a)−(b) shows the thermogravimetric (TG) curve and coke content of SAPO-34 samples after co-feeding reactions. It can be seen that the total coke amount rises when the carbon chain length of alkanes increases. The results of coked SSZ-13 samples (TOS = 258 min) are shown in Figure 14(c)−(d). All catalyst samples presented a two-stage mass loss characteristic: in the low-temperature region (300−450 ℃), it was attributed to the oxidation and removal of volatile coke precursors (such as methylbenzene, adamantane species); The high-temperature region (550−700 ℃) corresponds to the deep oxidation of insoluble polycyclic aromatic hydrocarbons (such as methyl naphthalene) and highly polymerized coke components. It is worth noting that the total coke content of the SSZ-13 samples with different reactants (Figure 14(d)) are similar which is correlated with high catalytic activity of SSZ-13. The differences in coke content of SAPO-34 and SSZ-13 originate from the effects of acidity differences on the formation and accumulation of reaction intermediates.

3 Conclusions

The coupled conversion of methanol and long-chain alkanes involves multi-path competitive reactions, including acid-catalyzed dehydration, hydrocarbon pool mechanism, hydrogen transfer and cracking-alkylation. Catalyst topology and the co-adsorbed species modulate the electronic properties of the active centers and the spatial confinement effects, resulting in significant differences in

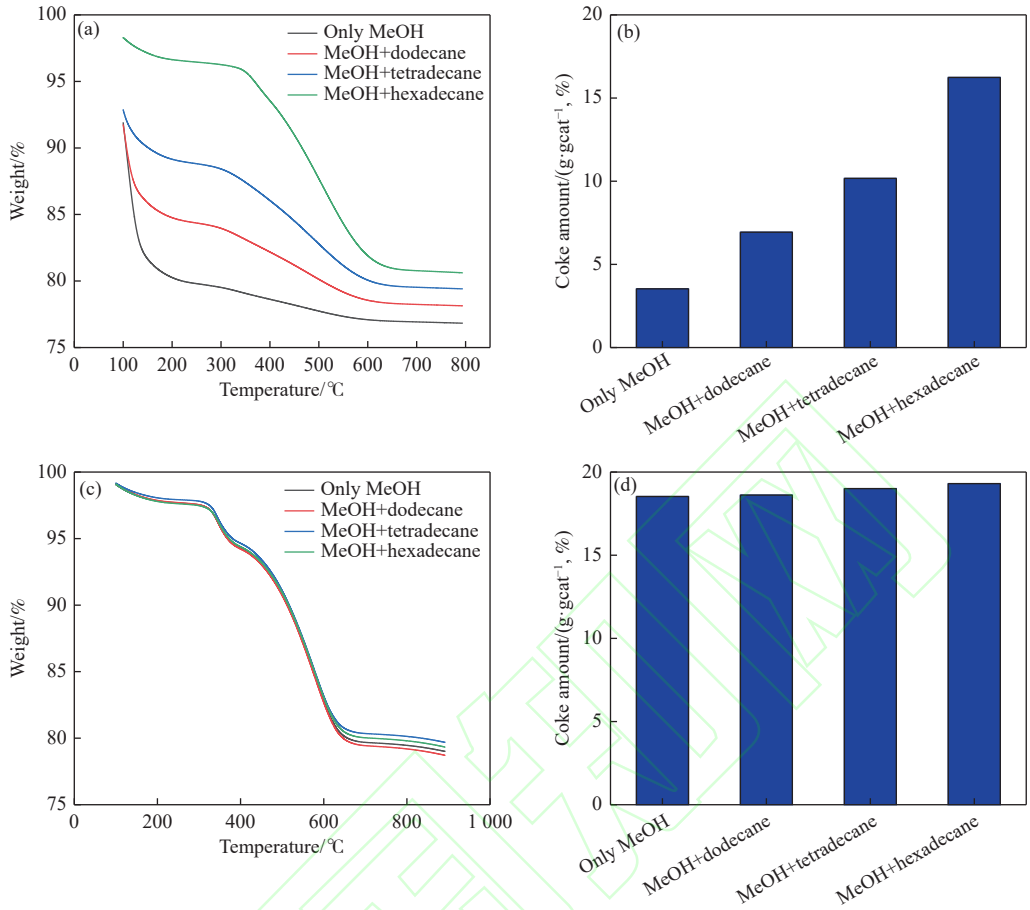

Fig. 14 TG analysis and total coke amount on spent CHA molecular sieves. (a) the TG curves and (b) the total coke amount of spent SAPO-34 with different reactants; (c) the TG curves and (d) the total coke amount of spent SSZ-13 with different reactants

the structure-activity responses of conversion and selectivity. At a specific reaction temperature of 250 ℃, co-feeding long-chain alkanes and methanol over SAPO-34 molecular sieve significantly enhances methanol conversion and shortens the induction period. Furthermore, carbon chain length exhibits a positive correlation with both conversions and low-carbon olefin (C_2-C_4) yields. In contrast, due to the acidic characteristics of SSZ-13, when the reaction temperature is reduced to 230 ℃, co-feeding long-chain alkanes with methanol similarly accelerates methanol conversion and reduces the induction period. Moreover, carbon chain length also positively correlates with conversions and C_2-C_4 olefin yields. Initially, the propylene/ethylene (P/E) ratio is high but gradually declines due to secondary hydrogen transfer reactions, yet remains above 1 throughout the reaction. Meanwhile, the co-feeding system of long-chain alkanes and methanol showed limited influence on the product distribution. It indicates that the channel shape-selective effect of the CHA molecular sieve dominates the product distribution. Its 8-membered ring channels have shape-selective advantages for propylene. The three-dimensional cross-channels maintains the intrinsic path of species evolution in the hydrocarbon pool through spatial confinement and does not significantly generate new reaction paths. The key retained species were identified through GC-MS analysis: polymethylbenzene and its protonated derivatives were mainly enriched in SSZ-13, while adamantane compounds and their methylation products were dominant in SAPO-34. The generation of these different species is closely related to the acid strength distribution of the catalysts and the pore confinement effect, directly regulate methylation, cyclization, and hydrogen transfer processes.

This study reveals that low-temperature long-chain alkane conversion promotes methanol transformation in CHA-structured molecular sieves, providing assistance for understanding the reaction mechanism during the induction period of methanol transformation.

Declaration of Competing Interest

The authors declare no conflict of interest.

References

[1] Laurendeau N M. Heterogeneous kinetics of coal char gasification and combustion[J]. Prog Energy Combust Sci, 1978, 4(4): 221−270.

[2] Wen W Y. Mechanisms of alkali-metal catalysis in the gasification of coal, char, or graphite[J]. Cat Rev -Sci Eng, 1980, 22(1): 1−28.

[3] Dahl I M, Kolboe S. On the reaction mechanism for propene formation in the MTO reaction over SAPO-34[J]. Catal Lett, 1993, 20(3): 329−336.
[4] Hickman D A, Schmidt L D. Production of syngas by direct catalytic oxidation of methane[J]. Science, 1993, 259(5093): 343−346.
[5] Dahl I M, Kolboe S. On the reaction mechanism for hydrocarbon formation from methanol over SAPO-34: I. Isotopic Labeling Studies of the Co-Reaction of Ethene and Methanol[J]. J Catal, 1994, 149(2): 458−464.
[6] Dahl I M, Kolboe S. On the reaction mechanism for hydrocarbon formation from methanol over SAPO-34: 2. isotopic labeling studies of the Co-reaction of propene and methanol[J]. J Catal, 1996, 161(1): 304−309.
[7] Sutton D, Kelleher B, Ross J R H. Review of literature on catalysts for biomass gasification[J]. Fuel Process Technol, 2001, 73(3): 155−173.
[8] Asadullah M, Ito, S, Kunimori, K, et al. Biomass gasification to hydrogen and syngas at low temperature: Novel catalytic system using fluidized-bed reactor[J]. J Catal, 2002, 208(2): 255−259.
[9] Bordiga S, Regli L, Cocina D, et al. Assessing the acidity of high silica chabazite H−SSZ-13 by FT-IR using CO as molecular probe: Comparison with H−SAPO-34[J]. J Phys Chem B, 2005, 109(7): 2779−2784.
[10] hongyuan L, juan L, ronghui W, et al. Synthesis of aluminum silicophosphate molecular sieve SAPO-34[J]. Petrochemical Technology, 1987, 16: 340−346.
[11] Liang J, Li H, Zhao S, et al. Characteristics and performance of SAPO-34 catalyst for methanol-to-olefin conversion[J]. Appl Catal, 1990, 64: 31−40.
[12] Chen D, Rebo H P, Moljord K, et al. Methanol conversion to light olefins over SAPO-34. sorption, diffusion, and catalytic reactions[J]. Ind Eng Chem Res, 1999, 38(11): 4241−4249.
[13] Liu Z, Liang J. Methanol to olefin conversion catalysts[J]. Curr Opin Solid State Mater Sci, 1999, 4(1): 80−84.
[14] Wilson S, Barger P. The characteristics of SAPO-34 which influence the conversion of methanol to light olefins[J]. Microporous Mesoporous Mater, 1999, 29(1): 117−126.
[15] Aguayo A T, Gayubo A G, Vivanco R, et al. Role of acidity and microporous structure in alternative catalysts for the transformation of methanol into olefins[J]. Appl Catal A: gen, 2005, 283(1-2): 197−207.
[16] Wei Y, Li J, Yuan C, et al. Generation of diamondoid hydrocarbons as confined compounds in SAPO-34 catalyst in the conversion of methanol[J]. Chem Commun, 2012, 48(25): 3082−3084.
[17] Wei Y, Yuan C, Li J, et al. Coke formation and carbon atom economy of methanol-to-olefins reaction[J]. ChemSusChem, 2012, 5(5): 906−912.
[18] Wei Y, Zhang D, Liu Z, et al. Methyl halide to olefins and gasoline over zeolites and SAPO catalysts: A new route of MTO and MTG[J]. Chinese. J Catal, 2012, 33(1): 11−21.
[19] CUIYU Y, YINGXU W, JINZHE L, et al. Temperature-programmed methanol conversion and coke deposition on fluidized-bed catalyst of SAPO-34[J]. Chinese J Catal, 2012, 33(2): 367−374.
[20] CUIYU Y, YINGXU W, LEI X, et al. Temperature-programmed methanol conversion on a microscale setup equipped with tapered element oscillating microbalance[J]. Chinese J Catal, 2012, 33(5): 768−770.
[21] Bleken F, Bjørgen M, Palumbo L, et al. The effect of acid strength on the conversion of methanol to olefins over acidic microporous catalysts with the CHA topology[J]. Top Catal, 2009, 52(3): 218−228.
[22] Qi L, Wei Y, Xu L, et al. Reaction behaviors and kinetics during induction period of methanol conversion on HZSM-5 zeolite[J]. ACS Catal, 2015, 5(7): 3973−3982.
[23] CHEN J, LI J, WEI Y, et al. Spatial confinement effects of cage-type SAPO molecular sieves on product distribution and coke formation in methanol-to-olefin reaction[J]. Catal Commun, 2014, 46: 36−40.
[24] TIAN P, WEI Y, YE M, et al. Methanol to olefins (MTO): From fundamentals to commercialization[J]. ACS Catal, 2015, 5(3): 1922−1938.
[25] ZHANG W, ZHANG M, XU S, et al. Methylcyclopentenyl cations linking initial stage and highly efficient stage in methanol-to-hydrocarbon process[J]. ACS Catal, 2020, 10(8): 4510−4516.
[26] REJMAN S, VOLLMER I, WERNY M J, et al. Transport limitations in polyolefin cracking at the single catalyst particle level[J]. Chem Sci, 2023, 14(37): 10068−10080.
[27] Rejman S, Reverdy Z M, Bör Z, et al. External acidity as performance descriptor in polyolefin cracking using zeolite-based materials[J]. Nat Commun, 2025, 16(1): 2980.

CHA 结构分子筛上甲醇与长链烷烃耦合反应

杨　闯[1,2]，王康军[1,*]，李金哲[1,2,*]，刘中民[1,2,*]

（1. 沈阳化工大学 化学工程学院, 辽宁沈阳 110142;
2. 中国科学院大连化学物理研究所 低碳催化技术国家工程研究中心, 辽宁大连 116023）

摘　要: 采用固定床微反装置研究了 CHA 结构分子筛催化甲醇和长链烷烃(正十二烷、正十四烷和正十六烷)的耦合反应, 发现在 SAPO-34 和 SSZ-13 分子筛上长链烷烃的引入均能促进甲醇的转化, 缩短反应诱导期。但在 CHA 催化剂上, 长链烷烃的引入对反应产物分布影响较小。积碳物种分析结果发现 SSZ-13 分子筛上多甲基苯及其衍生物是主要停留物种, SAPO-34 分子筛上金刚烷是主要积碳物种, 这表明积碳物种的生成主要与长链烷烃/甲醇耦合产物在分子筛酸位点的进一步转化相关。该研究为小孔 CHA 分子筛上长链烷烃的转化以及对反应诱导期内的甲醇转化反应的影响提供了支持。

关键词: 甲醇; 长链烷烃; 耦合反应; 诱导期; 分子筛
文献标识码: A

作者简介:

杨闯(1995), 硕士研究生, 研究方向为工业催化, y13940638662@163.com。

李金哲(1980), 博士, 研究员, 主要从事分子筛催化研究的研究工作, lijinzhe@dicp.ac.cn。

王康军(1979), 博士, 教授, 研究方向为能源资源转化催化材料构筑及其应用、精细化学品催化合成和产业化技术、功能材料设计制备及其应用, wangkj_dut@syuct.edu.cn。

刘中民(1964), 博士, 研究员, 主要从事能源化工领域应用催化研究与技术开发, iuzm@dicp.ac.cn。